Quantitative MRI Brain Studies in Mild Cognitive Impairment and Alzheimer's Disease: A Methodological Review

Stephanos Leandrou, Styliani Petroudi, *Member, IEEE*, Panayiotis A. Kyriacou, *Senior Member, IEEE*, Constantino Carlos Reyes-Aldasoro, *Senior Member, IEEE*, and Constantinos S. Pattichis, *Fellow, IEEE*

***Abstract*—Classifying and predicting Alzheimer's disease (AD) in individuals with memory disorders through clinical and psychometric assessment is challenging, especially in mild cognitive impairment (MCI) subjects. Quantitative structural magnetic resonance imaging acquisition methods in combination with computer-aided diagnosis are currently being used for the assessment of AD. These acquisitions methods include voxel-based morphometry, volumetric measurements in specific regions of interest (ROIs), cortical thickness measurements, shape analysis, and texture analysis. This review evaluates the aforementioned methods in the classification of cases into one of the following three groups: normal controls, MCI, and AD subjects. Furthermore, the performance of the methods is assessed on the prediction of conversion from MCI to AD. In parallel, it is also assessed which ROIs are preferred in both classification and prognosis through the different states of the disease. Structural changes in the early stages of the disease are more pronounced in the medial temporal lobe, especially in the entorhinal cortex, whereas with disease progression, both entorhinal cortex and hippocampus offer similar discriminative power. However, for the conversion from MCI subjects to AD, entorhinal cortex provides better predictive accuracies rather than other structures, such as the hippocampus.**

***Index Terms*—Alzheimer's disease (AD), classification, computer-aided diagnosis (CAD), entorhinal cortex, hippocampus, mild cognitive impairment (MCI), prediction, quantitative magnetic resonance imaging (MRI).**

Manuscript received July 7, 2017; revised November 24, 2017; accepted January 6, 2018. Date of publication January 23, 2018; date of current version July 24, 2018. This work was supported in part by the H2020-WIDESPREAD-04-2017-Teaming Phase 1, under Grant 763781, Integrated Precision Medicine Technologies. *(Corresponding author: Stephanos Leandrou.)*

S. Leandrou is with the Department of Health Sciences, European University Cyprus, 1516 Nicosia, Cyprus, and also with the School of Mathematical Sciences, Computer Science, and Engineering, City University of London, London EC1V 0HB, U.K. (e-mail: s.leandrou@euc.ac.cy).

S. Petroudi resides in Nicosia 1010, Cyprus (e-mail: stylianipetroudi@gmail.com).

P. A. Kyriacou and C. C. Reyes-Aldasoro are with the School of Mathematical Sciences, Computer Science, and Engineering, City University of London, London EC1V 0HB, U.K. (e-mail: p.kyriacou@city.ac.uk; reyes@city.ac.uk).

C. S. Pattichis is with the Department of Computer Science, University of Cyprus, 1678 Nicosia, Cyprus (e-mail: pattichi@ucy.ac.cy).

Digital Object Identifier 10.1109/RBME.2018.2796598

I. Introduction

DEMENTIA is a broad category of brain diseases that affect the brain by causing deterioration in memory, thinking, behavior, orientation, and, as a result, a decline in a person's daily functioning. Alzheimer's disease (AD) represents the most common form of dementia and may contribute to 60–80% of cases. Other common types include vascular dementia, Lewy body dementia, and frontotemporal dementia (FTLD) [1]. AD is most often diagnosed in people over 65 years of age, and it is the sixth leading cause of death in the USA. The greatest risk factors for AD are old age, family history, and the presence of Apolipoprotein e4 (ApoE4) gene in a person's genome. Currently, there is no specific cure for the disease, and the condition of the patient worsens with the disease progression eventually leading to death. According to Braak and Braak [2], the most evident change is the progressive deposition of abnormal proteins, both between and within the nerve cells. In the early stages, the most common symptom is difficulty in remembering recent events, while advanced AD patients often suffer from loss of the ability to take care of themselves, communicate with others, or even recognize their family members. Apart from challenging, the assessment and, most importantly, the early identification of the stage of AD are essential to provide a future treatment. Unfortunately, when the diagnosis is based exclusively on the clinical and psychometric assessment, a patient will be diagnosed with AD when the brain tissue has already undergone widespread and irreversible synaptic loss [3].

Mini-mental state examination (MMSE) [4] and clinical dementia rating (CDR) [5] are two of the most commonly used tests in the assessment of AD. MMSE consists of a series of clinical and psychometric assessment through neuropsychological tests, which assess language and memory abilities and the ability of solving problems. The maximum MMSE score is 30 points. A score less than 12 indicates severe dementia, 13–20 recommends moderate dementia, 20–24 suggests mild dementia, and 24–30 represents normal controls (NC). In parallel, CDR is used to describe memory, orientation, judgment, and problem solving, home and hobbies, and personal care. A score of 0 represents NC, 0.5 represents very mild dementia, 1 represents mild dementia, 2 represents moderate dementia, and 3 represents severe dementia. The revised criteria for the diagnosis of

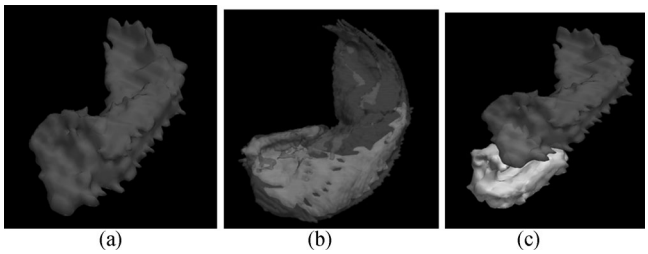

Fig. 1. Hippocampus and entorhinal cortex. (a) Hippocampus. (b) CA1 area within the hippocampus. (c) Entorhinal cortex with the hippocampus.

AD were proposed in 2007 by the National Institute of Neurological Disorders and Stroke–Alzheimer Disease and Related Disorders working group [6]. According to [6] and due to the uncertainty of clinical diagnosis, the clinical assessment should include at least one supportive feature:

1) medial temporal lobe (MTL) atrophy as seen in structural magnetic resonance imaging (MRI);
2) temporoparietal hypometabolism as seen in positron emission tomography (PET);
3) positivity on amyloid imaging as seen in PET;
4) abnormal neuronal cerebrospinal fluid (CSF) markers (tau and/or Aβ).

As a consequence of the AD, structural changes initiate within the MTL of the brain [7], a region that includes anatomically related structures that are essential for declarative memory [8]. Many postmortem studies [2], [9], [10] have implicated entorhinal cortex and the transentorhinal region as early sites of involvement in mild cognitive impairment (MCI) and in AD subjects. It was shown that the degenerative process initiates from the entorhinal cortex, followed by the hippocampus, the amygdala, and the parahippocampal gyrus [8], [11], [12]. With the disease progression, these regions lose neuronal tissue with consequent brain atrophy [13].

A definite diagnosis of AD relies on histological confirmation at postmortem biopsy [6], and brain inaccessibility has driven a search for diagnostic imaging markers. Imaging plays an important role in improving our understanding of AD, as it can provide an image of the brain of living patients that are affected by AD. Furthermore, imaging biomarkers can be used for differential diagnosis due to the uncertainty of clinical tests in differentiating other subtypes of dementia such as FTLD [14], [15]. The entorhinal cortex and the hippocampus (see Fig. 1) are the two most common regions of interest (ROIs) used in both *in vivo* and postmortem investigations on the pathophysiology in AD. However, a visual qualitative assessment of MRI is not enough to estimate the rate of the tissue loss in the areas affected by the disease, and quantitative measures are essential for the assessment of the disease. Furthermore, the human eye cannot perceive the minimum degree of atrophy, and without quantitative measurements, image evaluation is subjective. On the other hand, by using only MMSE tests, MCI, which represents a transitional period between normal ageing and clinical probable AD, cannot be easily identified through cognitive tests, mainly because these subjects do not have severe memory problems [6]. As the size of the MRI datasets increases and manual tracing is much more time consuming, computer-aided diagnosis (CAD) systems can outline the areas of interest, usually by automated or semiautomated techniques, and can provide quantitative measurements.

TABLE I
OPEN SOURCE IMAGING DATA FOR AGING

Name	Subjects	Data
Alzheimer's Disease Neuroimaging Initiative (ADNI) http://adni.loni.usc.edu/	483 NC, 300 eMCI, 300 lMCI, 550 MCI, 350 AD	Clinical and cognitive assessments, MRI, PET, genetic, biospecimen
Australian Imaging Biomarker and Lifestyle flagship (AIBL) https://aibl.csiro.au/	768 NC, 133 MCI, 211 AD	Clinical and cognitive assessments, MRI, PET, biospecimen, dietary/lifestyle assessment
Open Access Series of Imaging Studies (OASIS) http://www.oasis-brains.org/	73 NC, 14 ADc, 64 AD	MRI
AddNeuroMed http://www.innomed-addneuromed.com	232 NC, 225 MCI, 259 AD	Clinical and cognitive assessments, blood, MRI

GLOSSARY: NC: normal controls; eMCI: early mild cognitive impairment; lMCI: late mild cognitive impairment; MCI: mild cognitive impairment; AD: Alzheimer's disease; ADc: subjects who converted to AD; MRI: magnetic resonance imaging; PET: positron emission tomography.

This review describes the overall results, including accuracy, specificity, and sensitivity of the image-processing methods that assess AD as observed in structural MRI. Additionally, it describes the effectiveness of these methods in the prediction of conversion from MCI to AD. The rest of this review is organized as follows. Section II presents the CAD system pipeline and Sections III and IV present the use of CAD systems in the diagnosis and prognosis of the disease, respectively. Section V concludes which methods and structures are suggested for both diagnosis and prognosis of AD. Section IV addresses and suggests future directions for the assessment of AD.

II. CAD System Pipeline

The objective of CAD systems is to assist the radiologist in the interpretation of medical images as a supporting tool. Furthermore, CAD provides quantitative information for ROIs to produce accurate and complete pathology reports. In medical image analysis, the following steps, i.e., image acquisition and preprocessing, ROI segmentation, feature extraction, classification, and interpretation, are usually carried out to provide quantitative measurements of biomedical images. Medical image analysis steps and techniques used for the development of CAD systems for the assessment of dementia are analyzed in this section.

A. Datasets and Preprocessing

In AD research, many investigators obtain their data from online databases (see Table I). These databases provide researchers with study data to define the progression of AD. One of the most comprehensive databases is the Alzheimer's Disease Neuroimaging Initiative (ADNI) [16], an ongoing, longitudinal, multicenter study. The ADNI was launched in 2003

as a public–private partnership, led by a principal investigator Michael W. Weiner, MD. The primary goal of the ADNI has been to test whether serial MRI, PET, other biological markers, and clinical and neuropsychological assessment can be combined to measure the progression of MCI and early AD. The ADNI image processing pipeline includes postacquisition correction of gradient warping (Gradwarp) [17], B1 nonuniformity correction [18] depending on the scanner and coil type, and phantom-based scaling correction [19]. For up-to-date information, see http://adni.loni.usc.edu/. Apart from the ADNI, the Australian Imaging Biomarker and Lifestyle flagship study of aging (http://aibl.csiro.au) has already enrolled 1100 participants and collected over 4.5 years' worth of longitudinal data. The Open Access Series of Imaging Studies (OASIS) [20] provides data to be used in the determination of diagnostic markers for the assessment of AD and the data are divided in two sets: the cross-sectional MRI data in young, middle aged, nondemented and demented older adults and the longitudinal MRI data in nondemented and demented older adults. AddNeuroMed [21] is a cross European public/private consortium developed for AD biomarker discovery. It combines modalities, and it uses animal models in biomarker research.

Furthermore, two large dementia challenges where research groups could test and compare their algorithms in the AD assessment are the CADDEMENTIA [22] (http://caddementia.grandchallenge.org) and the Alzheimer's Disease Bid Data DREAM challenge (http://dreamchallenges.org).

B. ROI Segmentation

The role of segmentation in medical imaging is to separate an image into regions to study anatomical structures, to identify ROIs, or to measure the volume of a tissue. For the automatic segmentation of gray matter (GM), white matter (WM), and CSF from magnetic resonance (MR) images, three methodologies have been proposed: statistical-based segmentation methods, learning-based segmentation methods, and atlas-based segmentation methods. Atlas-based segmentation methods are the most frequently used in medical image segmentation. In atlas-based segmentation, an intensity template is registered nonrigidly to a target image, and the resulting transformation is used to propagate the tissue class or anatomical structure labels of the template into the space of the target image [23]. The study by Babalola *et al.* [24] compared atlas-based and model-based segmentation techniques and was tested on 270 subjects. The two atlas-based methods, classifier fusion and labeling and expectation-maximization segmentation using a dynamic brain atlas, performed significantly better than the model-based methods, profile active appearance models, and Bayesian appearance models. Factors that affect accuracy in multiatlas segmentation are presented in [23].

Based on the aforementioned segmentation methods, several software "pipelined" image analysis packages for automated brain tissue segmentation have been developed (see Table II). These packages usually contain skull stripping, intensity nonuniformity correction, and automated segmentation. FreeSurfer (Martinos Center for Biomedical Imaging, Harvard-MIT, Boston, MA, USA) [25] is an open-source software suite for processing and analyzing brain MRI images. It represents one of the most commonly used software packages in image analysis, and it segments MRI scans automatically using a Bayesian approach [26]. Morey *et al.* [27] compared automated segmentation methods and hand tracing of the hippocampus, and it was shown that Freesurfer is preferable compared to FSL/FIRST (Functional MRI Brain—FMRIB Software Library, abbreviated as FSL—FMRIB Integrated Registration and Segmentation Tool, Oxford University, Oxford, U.K.) [28]. The statistical parameter mapping software (Wellcome Trust Centre for Neuroimaging, Institute of Neurology, UCL, London, U.K.) is a freely available suite of MATLAB used for segmentation, normalization, registration, volume measurements, and other useful image analysis steps.

TABLE II
SELECTED BRAIN SEGMENTATION SOFTWARE PACKAGES

Name	Description	Studies
FreeSurfer	Open source software suite for processing and analyzing (human) brain MRI images https://surfer.nmr.mgh.harvard.edu/	[25], [27], [30], [31], [31]–[35]
Statistical parameter mapping (SPM)	MATLAB software package implementing statistical methods for analysis of functional and structural neuroimaging http://www.fil.ion.ucl.ac.uk/spm/	[36]–[46]
LONI pipeline	Includes workflows that take advantage of all widely used tools available in neuroimaging, genomics, bioinformatics, etc. http://pipeline.loni.usc.edu/	[29], [32], [47]–[49]

The LONI Pipeline [29] is a graphical workflow environment, which allows grid utilization and provides a significant library of computational tools. It was built to be used in complex neuroimaging analysis, which requires deep knowledge about the input/output requirements of algorithms. The LONI Pipeline could be used to design, execute, validate, and deliver complex heterogeneous computational protocols.

C. Feature Extraction

Thus, through feature extraction, it is possible to retrieve important data that can assist the characterization of a pathology. Feature extraction methodologies analyze objects or images to extract the most prominent features that are representative of the various classes of objects.

Table III lists selected methods that are currently used in the assessment of AD as described in [30], where these methods were compared. According to Cuingnet *et al.* [30], these approaches can be divided into three categories, depending on the type of features extracted from the MRI:

1) voxel based, if the features are derived from GM, WM, or CSF;
2) vertex based, if the features are derived from the cortical surface such as thickness measurements;
3) ROI based, if the features are derived from ROIs.

However, apart from the hippocampus, it should be noted that the entorhinal cortex is also a structure currently used

TABLE III
SUMMARY OF STRUCTURAL MRI FEATURES BASED ON [30]

Category	Subcategory	Tissue	Description	Studies
Voxel based	Direct	GM	Probability maps of voxels of the tissue directly as features in the classification	
		GM+WM+CSF		
	STAND-score	GM, WM, and CSF tissue probabilities	Selection steps and a sequence of feature aggregation is used to reduce dimensionality.	[37], [38]
	Atlas based	Mean tissue probabilities	Uses labeled atlas to group the voxels into anatomical regions	
	COMPARE	GM	Creates homogeneously discriminative regions, in which the voxel values are aggregated to form the features of the classification	
		GM+WM+CSF		
Cortical Thickness	Direct	-	Consists cortical thickness values at every vertex directly as features	[37]
	Atlas based	-	Vertices are grouped into anatomical regions using an atlas	[31], [66]
	ROI	Hippocampus, entorhinal cortex, supramarginal gyrus	Measures the cortical thickness in specific areas	[31]
Volume and Shape	Hippocampus and Entorhinal cortex	-	Discriminative power of the hippocampus and entorhinal cortex only	[16], [39], [40], [49]–[53], [41], [54]–[56]

GLOSSARY: STAND: structural abnormality index; ROI: region of interest; GM: gray matter; WM: white matter; CSF: cerebrospinal fluid.

by many studies for the assessment of AD. In this review, structural MRI features derived from voxel-based morphometry (VBM), cortical thickness, volume, shape, and texture are described.

In the assessment of AD, VBM has the advantage examining the whole brain and not a particular structure. Specifically, it detects differences in the local composition between different brain tissue types such as GM and WM [50]. First, the brain images are segmented into their three main tissue components, GM, WM, and CSF and, then, are spatially normalized to the same stereotactic space. This allows different brains to be compared directly through a voxelwise statistical analysis over the entire brain. For technical and methodological information about VBM, the reader is referred to [51]. Nowadays, VBM is used to examine the whole volume of the brain and to detect differences or similarities in images for two populations [52]. Furthermore, it is also used to calculate cortical thickness changes on the entire cortex. A limitation of thickness measurements is that they cannot detect changes on subcortical structures such as WM or CSF; therefore, it is only used to detect the regional distribution of cortical atrophy. In general, some of the limitations of VBM include systematic registration errors during spatial normalization [53] and difficulties in detecting WM changes in T1 MRI sequences or pathologies that are not common in the majority of a population [54].

Volumetric techniques are used to measure the volume of a structure; however, a major weakness of volume analysis is that the thickness or shape of a structure might change before its volume. According to [55], global hippocampal volumetry might not be always sensitive enough to follow changes within a single population, which may reflect conversion from a healthy state or disease progression. In differential diagnosis, VBM showed higher accuracy from volume measurements, in the ability to differentiate AD from FTLD [14], [15].

Shape analysis is used in digital geometric models of surfaces and/or volumes of objects of interest in order to detect similarities or differences between the objects [56]. It examines the shape of a structure that gives not only more sensitivity to follow the progression of the atrophy, but also allows its evaluation in different subfields. Among the many techniques [56] used to obtain shape features of the human brain, corresponding spherical harmonic description (SPHARM), deformation-based morphometry, and deformable models are the methods mainly used, mainly due to alignment factors.

Texture is an indistinct concept often attributed to human perception of variation of the color/intensity of a surface, quantifying properties such as smoothness, coarseness, and regularity. It could be argued that texture refers to the spatial and statistical relationship of pixel values in an ROI. The early stage of AD is associated with small-scale changes in terms of neurofibrillary tangles (NFTs) and amyloid-β (Aβ) plaque deposition [57]. According to Castellano *et al.* [58], these small-scale changes are able to form certain textural patterns in MRI images recognizable by extracting texture descriptors from the image. In AD, texture analysis is less used than the other methods. However, the information provided by texture analysis cannot be visible through volume and shape properties [36]; thus, it may have the advantage of detecting earlier microscopic alterations [58]. Broadly, the approaches used to describe texture features in neuro MRI can be split into *syntactic, statistical*, and *spectral* [59].

Statistical-based approaches (see Table IV) are mostly used, and they represent the texture indirectly by nondeterministic properties that prescribe the distributions and relationships between grey levels of an image [59]. According to Kovalev *et al.* [60], 3-D texture features contain more spatial information, higher sensitivity, and specificity compared to 2-D techniques. Three-dimensional texture features include the use of

TABLE IV
SELECTED 2-D TEXTURE FEATURES IN THE EVALUATION OF MCI AND AD

Category	Subcategory	Tissue	Description	Features	Studies
Statistical	First-order gray level	-	Contain information related to the gray-level distribution of an image.	Variance, skewness, kyrtosis, mean, gradient	[76]
	Second-order co-occurrence matrix (GLCM)	Whole brain, hippocampus, entorhinal cortex	Describe how often 2 pixels with different values appear in the field of view separated by a distance d in direction θ (0°, 45°, 90°, and 135°)	Angular second moment, contrast, correlation, sum of squares, inverse different moment, sum average, sum variance, sum entropy, entropy, difference variance, information measures of correlation.	[36], [77]–[84]
	Second-order run-length matrix (RLM)	-	Contain information about spatial relationships between groups of pixels having similar gray level values.	Short runs emphasis, long runs emphasis, gray-level non-uniformity, run-length nonuniformity, run percentage	[78], [83]–[85]

TABLE V
CLASSIFICATION TECHNIQUES USED IN CAD MCI AND AD SYSTEMS

Classifier	Description	Studies
Discriminant analysis [91] [93]	Predict classification in a group based on continues variables	[31], [66], [68], [72], [77], [94], [95]
Logistic regression [96]	It examines relationships between a categorical Y and a continuous X variable	[81], [97]
Neural networks	Fit nonlinear models using nodes and layers. Could be very good predictors	[78]
Support vector machines [89], [98]	Supervised, multivariate learning methods used for classification, as well as regression	[32], [36]–[38], [40], [41], [75], [99]

law filters [61], run-length matrices (RLMs) [62], subband [63], [64], Gaussian–Markov random fields, and a combination of co-occurrence matrices and Gabor filters [63]. For a review on the 3-D texture, the reader is referred to [65].

D. Classification Methods

Classification is used for the identification of patterns features of interest into the classes they belong. Moreover, machine-learning techniques have the potential to classify MR features without requiring a priori hypotheses from where this information may be coded in the images [86]. When classifiers are used, image samples are divided into two sets: training and testing [87]. The most popular statistical techniques used in CAD include discriminant analysis (DA), logistic regression (LR), neural networks, and support vector machine (SVM). These techniques are presented in Table V.

When the sample size is large, linear DA and LR have similar results, whereas in smaller samples, DA performs better. Furthermore, DA is faster compared to LR. Regardless of the data distribution, LR performs well, and it should be used as the first choice to classify data [88]. On the other hand, DA is preferred when the variables are categorized and as long the assumptions are met. Furthermore, DA is preferred when the number of categories is big enough to let the estimated mean and variance be close to the population values of the continuous explanatory variables [88].

SVMs were developed by Vapnik [89], and they represent pattern recognition algorithms based on training, testing, and performance evaluation. Compared to DA that is a more generative method as it focuses on all data points, SVMs are more discriminative as they concentrate on the points that are difficult to classify. They can be used when the data have an unknown distribution [90], and one of their strongest advantages is that they provide excellent results in pattern recognition and good generalization performance. Furthermore, they offer a possibility to train generalizable nonlinear classifiers in high-dimensional spaces using a small training set [91].

Neural networks can be used as an alternative to LR. Artificial neural networks (ANNs) benefit from the availability of multiple training algorithms; they require less statistical training and perform well in predicting medical outcomes. Limitations of ANNs include computational load, restricted potential to unmistakably detect possible causal relationships, and overfitting suffering [92].

III. COMPUTER-AIDED SYSTEMS FOR THE DIAGNOSIS OF ALZHEIMER'S DISEASE

Table VI tabulates CAD systems for the classification of MCI and AD. Quantitative MRI studies tabulated in the following are based on amyloid, volume, thickness, shape, and texture analysis that are described in the following subsections. For each study, the main author, ROI, data type, the number of subjects and classification accuracy, sensitivity, and specificity are given.

A. Quantitative MRI Studies Based on VBM

VBM describes global changes or atrophy of deep cerebral structures. Evans *et al.* [100] revealed a mean standard deviation whole-brain loss at 1.5% per year in AD patients compared to 0.5% per year in NC. On the other hand, MCI subjects had an intermediate rate of 1.1% loss per year. Interestingly, in this study, it was noticed that MCI patients who converted to AD had brain atrophy twice more than the MCI patients who did not progress to AD.

Busatto *et al.* [101] used a fully automated VBM technique to evaluate GM abnormalities over the entire area of the temporal lobe in the classification of NC subjects from AD patients. Their results confirmed the findings of previous ROI-based studies [11], [102], [103], where significant GM loss was detected bilaterally in the MTL region in AD patients. The entorhinal

TABLE VI
SELECTED QUANTITATIVE MRI STUDIES IN THE CLASSIFICATION OF MCI AND AD SUBJECTS

Study	ROI	Data type	Subjects	Classification	Acc.	Se.	Sp.
Klöppel *et al.* [37]	GM	VBM	20 NC, 20 AD	NC versus AD	90%	85%	95%
				NC versus AD	84%	84%	84%
Colliot *et al.* [39]	Hip.	Volume	25 NC, 24 MCI, 25 AD	NC versus MCI	66%	66%	65%
				MCI versus AD	82%	83%	83%
Juottonen *et al.* [68]	Hip. & Erc.	Volume	32 NC, 30 AD	NC versus AD	Hp.: 86%	80%	91%
					Erc.: 87%	80%	94%
Pennanen *et al.* [72]	Hip. & Erc.	Volume	48 AD, 65 MCI, 59 NC	NC versus AD	91%	88%	93%
				NC versus MCI	66%	66%	65%
				MCI versus AD	82%	81%	83%
			49 NC, 48 MCI			74%	94%
Desikan *et al.* [31]	Erc. Supramarginal gyrus	Thickness	94 NC, 57 MCI	NC versus AD	NA	90%	91%
					75%	79%	71%
Lerch *et al.* [94]	Entire cortex	Thickness	17 NC, 19 AD	NC versus AD	94%	94%	95%
	Parahippocampal Gyrus			NC versus AD	94%	96%	92%
Gerardin *et al.* [41]	Hip.	Shape	23 NC, 23 MCI 25 AD	NC versus MCI	83%	83%	84%
Ferrarini *et al.* [75]	Hip.	Shape	50 NC, 15 MCI-c, 15 MCI-non-c, 50 AD	NC versus AD	90%	92%	NA
				MCI versus AD	80%	80%	NA
Freeborough and Fox [77]	Whole brain	Texture	40 NC, 24 AD	NC versus AD	91%	79%	100%
Zhang *et al.* [78]	Hip., Erc. & CSF	Texture	17 NC, 17 AD	NC versus AD	64–96%	NA	NA
Simoes *et al.* [36]	Whole brain	Statistical texture maps	15 NC, 15 MCI	NC versus MCI	87%	85%	95%

GLOSSARY: Acc: accuracy; Se: sensitivity; Sp: specificity; AUC: area under curve; NC: normal controls; MCI: mild cognitive impairment; MCI-non-c: MCI nonconverters; AD: Alzheimer's disease; GM: gray matter; CSF: cerebrospinal fluid; Hip: hippocampus; Erc: entorhinal cortex; VBM: voxel-based morphometry.

cortex was found to be the primary region where the neurodegenerative changes initiate in the earliest stages of AD.

Karas *et al.* [34] used VBM, and apart from the earlier findings in the atrophy of the hippocampus, they demonstrated global reduced GM volume including the cerebellum, medial thalamus, and head of the caudate nucleus as well of the cingulum in AD patients. Their findings collated with the histopathological staging of Braak *et al.* [9], [104]. Another study by Karas *et al.* [105] analyzed the patterns of GM loss in order to examine what characterizes MCI and what determines the differences with AD by using VBM methods. Apart from quantifying the extent of GM loss between MCI subjects and AD patients, the authors wanted to investigate if the hippocampal volume still changes in patients who converted to AD. The results of the study showed that MCI patients had GM loss in the MTL area, where the parietal and cingulate cortices were areas more related to AD patients. Whitwell *et al.* [42] compared the pattern of GM loss in MCI patients who progressed to AD within a fixed time of period (18 months from baseline scan) with the subjects who remained stable. Compared to NC, the subjects that progressed to AD had bilateral GM loss in specific regions of the brain. Interestingly, the nonprogressed MCI patients had no areas of GM loss when compared to the NC. Thus, the VBM method might not be the most sensitive technique for the classification of normal and MCI patients. However, when the two groups (stable and progressed MCI) were directly compared, the progressed group showed more GM atrophy.

Klöppel *et al.* [37] used a voxel-based SVM approach to analyze the GM of NC and AD patients through modeling two different anatomical areas: in the first model, they used data from the whole brain, and on the second, they used data from a hippocampus-centered ROI. Their method reached an accuracy of 90% when evaluated on 20 NC and 20 AD subjects.

B. Quantitative MRI Studies Based on Volume Analysis

Several studies used hippocampal volumetric measurements and confirmed that hippocampal atrophy can constitute a useful diagnostic biomarker. The studies that used AD patients and NC from the ADNI database reported that the hippocampal volumes were varying between 1600 mm^3 [106] and 3000 mm^3 [107]. According to the study by Schuff *et al.* [106], the hippocampal loss was accelerated by 26.5 ± 4.5 $mm^3/year^2$ in AD and 12.1 ± 3.2 $mm^3/year^2$ in MCI, equivalent to $-1.6 \pm 0.2\%/year^2$ and $0.6 \pm 0.2\%/year^2$, respectively, relative to baseline volume.

One of the first studies where MRI was used to investigate if volumetric measurements in MTL could provide information for the classification of NC and AD patients took place in 1997, by Jack *et al.* [108]. Their study included 126 NC subjects and 94 probable AD patients, where they estimated volume measurements of hippocampus, parahippocampal gyrus, and the amygdala. Their results showed a parallel structure decline with increasing age in control subjects for both women and men, and in each case, MTL volume in AD patients was significantly smaller compared to NC subjects ($p < 0.001$). The MTL structure, which performed better for this classification, was the hippocampus. In 2001, Galton *et al.* [67] confirmed that hippocampal atrophy is a useful diagnostic biomarker, and they showed that there was a 50% hippocampal atrophy in AD patients.

In [39], Colliot *et al.* used hippocampal volume to distinguish NC from MCI and AD patients. The technique used was previously used by Chupin *et al.* [109], and it was fully automated

where both the hippocampus and amygdala were segmented at the same time. The results of their study revealed significant hippocampal volume reductions in all groups of patients. Specifically, there was a 32% volume reduction between AD and NC, a 19% reduction between MCI and NC, and, finally, a 15% reduction between AD and MCI.

Apart from hippocampus, other structures such as entorhinal cortex are used for the assessment of AD. However, because it is controversial whether entorhinal cortex or hippocampus is more affected with the disease progression, the study by Juottonen *et al.* [68] used volumetric MRI on AD patients and NC subjects to investigate which of the two structures was more affected. Both structures had the ability to differentiate AD patients from NC subjects, and no essential difference was found between the discriminative power of entorhinal cortex and hippocampal volumes. Specifically, the volume of entorhinal cortex in AD patients was 38% less on the right and 40% less on the left side, compared to NC subjects. A similar pattern of atrophy was noticed on the hippocampal volume, where it was 33% less on the right and 35% less on the left side compared to NC subjects. Obviously, in the late states of the disease, both structures have a similar atrophy rate.

According to Pennanen *et al.* [72], the appropriate ROI selection should depend on the classification group. Thus, they investigated which structures of the brain can be used to best classify the three different study groups. Their results showed that entorhinal cortex atrophy was more severe, in comparison with hippocampus volume, in MCI subjects, whereas, in AD patients, the hippocampal atrophy was more pronounced. Specifically, the best overall classification (66%) between MCI and NC subjects was achieved with entorhinal cortex, whereas the best overall classification (82%) between MCI and AD patients and between NC and AD patients (91%) was achieved with hippocampal volume. Similar to [68], the left hippocampal atrophy appears to be more severe for all the subjects.

C. Quantitative MRI Studies Based on Thickness Analysis

Desikan *et al.* [31] carried out automated structural measurements of entorhinal cortex and supramarginal gyrus thickness in order to differentiate MCI subjects and AD patients from normal patients. They used baseline volumetric scans from two independent cohorts, where images were obtained from the OASIS [20] and the ADNI database [16]. Hippocampal volume, entorhinal cortex, and supramarginal gyrus thickness indicated an average area under curve (AUC) of 0.91 in the training cohort and an AUC of 0.95 in the validation cohort. It should be mentioned that their results were comparable or even more accurate from nuclear medicine techniques such as fluorodeoxyglucose (FDG)-PET [110], [111] or amyloid-binding PET studies [112], [113]. Furthermore, discrimination accuracy of MCI subjects in this study was comparable to one prior PET study utilizing a radioactive amyloid and tau protein tracer [113] and two MRI studies [95], [114].

Lerch *et al.* [94] used an automated method to measure the cortical thickness across the entire brain and detect differences between AD patients and NC. Cortical thickness was declined in many areas of the brain; however, the parahippocampal gyrus and the MTLs were the areas most affected. Similarly to other studies [68], [72], it was found that the left side of the brain was more severely affected. Therefore, according to this study, cortical atrophy in the early stages of AD is not related only to MTL but to the limbic system, the lateral temporal lobes, and cortex as well.

D. Quantitative MRI Studies Based on Shape Analysis

Gerardin *et al.* [41] used hippocampal shape features instead of volume analysis, and specifically, SPHARM coefficients were used to model the hippocampal shape. Their results revealed that shape analysis can detect local atrophy on the hippocampus, before it starts losing volume. Therefore, this technique may be more sensitive and in particular at the MCI stage. Shape analysis can be used to reveal atrophy on local and nonglobal areas of the hippocampus, and according to the authors, the classification accuracy between AD patients and NC subjects was superior to studies that used volume analysis where classification accuracy was ranging from 80% to 90%. Furthermore, when MCI patients were involved in volume studies, the discriminative power was even lower, ranging from 60% to 74%. However, these results were reported in volume studies where manual and not automated segmentation was used.

Chételat *et al.* [43] conducted a longitudinal study where MCI subjects were followed for 18 months. Their purpose was to project possible atrophy maps onto a 3-D surface view of the hippocampus between MCI patients who converted or not to AD, compared to the profile of GM loss across normal aging. Their results showed that atrophy was more significant in converters than in nonconverters, and this effect was more marked at follow-up. Interestingly, for both converters and nonconverters, the hippocampal atrophy was more evident on the superior-lateral part of the hippocampus, called CA1. Histopathological studies [115] also agreed that there was a relatively higher degree of atrophy in that specific hippocampal subfield. Similar results were observed by Apostolova *et al.* [74]. On the other hand, GM loss with increasing age was more severe on the inferior part of the hippocampus corresponding to the subiculum, something that was reported by Frisoni *et al.* [116] as well. Ferrarini *et al.* [75] used hippocampal shape-based markers in the CA1 region, and by using SVMs on either one or both hippocampi, they discriminated AD patients from NC subjects with an overall accuracy of 90%, and stable MCI subjects from MCI converters with an accuracy of 80%.

E. Quantitative MRI Studies Based on Texture Analysis

Freeborough and Fox [77] used texture analysis for the classification of AD patients from NC. They extracted features by using gray-level co-occurrence matrices for offset angles of 0^{o}, 45^{o}, 90^{o}, and 135^{o}. From each matrix, they derived 13 features, and the mean and range of each feature over the four offset angles were completed. They indicated that texture analysis can reveal significant different values between NC and AD patients.

TABLE VII
SELECTED QUANTITATIVE MRI STUDIES IN THE PREDICTION OF CONVERSION FROM MCI TO AD

Study	ROI	Data type	Follow-up (months)	Converters/Total MCI	Acc.	Se.	Sp.
Davatzikos *et al.* [44]	Whole brain	VBM	0–36	69/239	56%	95%	38%
Misra *et al.* [99]	Whole brain	VBM	0–36	27/103	82%	NA	NA
Plant *et al.* [45]	Whole brain	VBM	0–30	9/24	75%	56%	87%
Duchesne *et al.* [122]	MTL	VBM	0–28	11/31	81%	70%	100%
Koikkalainen *et al.* [123]	Whole brain	TBM	0–36	154/369	72%	77%	71%
Chupin *et al.* [40]	Hip. & Amygdale	Volume	0–18	76/210	64%	60%	65%
deToledo-Morrell *et al.* [97]	Hip. & Erc.	Volume	0–36	10/27	93%	NA	NA
Killiany *et al.* [12]	Erc.	Volume	0–36	13/73	84%	NA	NA
Devanand *et al.* [126]	Hip. & Erc.	Volume	0–36	37/139	88%	83%	NA
Killiany *et al.* [95]	Erc., STS	Volume	0–36	19/79	93%	95%	90%
Querbes *et al.* [66]	Cortex	Thickness	0–24	72/122	73%	75%	69%
Eskildsen *et al.* [128]	Cortex	Thickness	0–36	-	67–76%	NA	NA
Bakkour *et al.* [35]	Cortex	Thickness	0–30	20/49	NA	83%	65%
Desikan *et al.* [130]	Neocortex	Thickness & Volume	0–36	TC: 60/162	AUC: 0.82	74%	84%
				VC: 58/162	AUC: 0.84	87%	66%
Ferrarini *et al.* [75]	Hip.	Volume	0–33	15/30	73%	63%	77%
		3D Shape			80%	80%	80%
Costafreda *et al.* [32]	Hip.	3D Shape	0–12	22/103	80%	77%	80%
Cuingnet *et al.* [30]	Whole brain	VBM	-	-	71%	77%	78%
-	Hip.	Atlas based	0–18	76/210	67%	62%	69%
-	Cortex	Thickness	-	-	70%	32%	91%
Wolz *et al.* [129]	Whole brain	TBM	-	-	64%	65%	62%
-	Whole brain	Manifold-based learning	-	-	65%	64%	66%
-	Hip.	Atlas based	0–48	167/405	65%	63%	67%
-	Cortex	Thickness	-	-	56%	63%	45%
-	Combination	Combination	-	-	68%	67%	69%
Sørensen *et al.* [81]	Hip.	Texture	0–12	-	AUC: 0.74	NA	NA
		Texture & Volume	0–24		AUC: 0.74		

GLOSSARY: ROI: region of interest; MCI: mild cognitive impairment; VBM: voxel-based morphometry; TBM: tensor-based morphometry; Acc: accuracy; Se: sensitivity; Sp: specificity; MTL: medial temporal lobe; Hip.: hippocampus; Erc.: entorhinal cortex; STS: superior temporal sulcus; TC: training cohort; VC: validation cohort; AUC: area under curve.

Zhang *et al.* [78] used 3-D texture features to identify NC from AD patients. Over 100 texture features were extracted from spherical ROIs placed within the area of the hippocampus and the entorhinal cortex, using image histograms, gradients, co-occurrence matrices, and RLMs. To investigate the impact on the ROI selection, they placed 3-D ROIs in three ways. The ROI that performed better included the regions of hippocampus and entorhinal cortex and part of CSF. The selection of a larger ROI, which in this case included a part of the CSF, generated a higher classification accuracy. They achieved the highest accuracy mentioned in the literature, maybe due to the fact that they used severely affected AD subjects.

de Oliveira *et al.* [79] applied texture analysis on MCI subjects. In their analysis, they choose to use the thalamus and calossal due to their anatomic heterogeneity, which is more suitable for texture analysis. The analysis was carried out separately for the two ROIs using manual segmentation and the MaZda tool [117] to extract the features. According to the authors, this method was more reliable than other techniques [77], [118], [119], where the whole-brain texture was analyzed. The objective of their study was to classify NC from amnestic MCI subjects and mild AD patients, and through their analysis, they revealed differences between the thalamus and corpus callosum, which differentiated the two groups of subjects.

Simoes *et al.* [36] used a whole-brain approach by applying local statistical texture maps for the classification of MCI subjects from NC. Through SVM, they achieved a mean accuracy of 87%. However, their sample was small ($N = 30$). In the study by Sørensen *et al.* [81], the classification capabilities of hippocampal texture were evaluated using receiver operating characteristic curves with the corresponding AUC as performance measure. Texture analysis had an AUC of 0.912 in discriminating NC versus AD and 0.764 between NC versus MCI. For the same groups, the AUC curves for volume analysis were 0.909 and 0.784, respectively. To the best of our knowledge, this is the only study that evaluated if there is a correlation between texture and the volume of the hippocampus in MCI subjects. Regarding prognosis, it was shown that the hippocampal texture is superior rather than volume measurements with an AUC of 0.74 versus 0.67, respectively, and their results were correlated with FDG-PET.

IV. PREDICTION OF CONVERSION FROM MCI TO AD

Recently, the task of predicting conversion from MCI to AD has received a lot of attention, mainly because, nowadays, large multicenter studies, such as the ADNI, provide longitudinal data to the research community. The MCI term was first introduced in the literature by Reisberg *et al.* [120] in 1988, and two decades later, Farias *et al.* [121] showed that a 10–15% rate of MCI subjects will progress to dementia. The biggest challenge in AD assessment is to predict if a patient will develop the disease. The identification of these patients is of great importance as they will be provided earlier with possible preventive pharmaceutical (or nonpharmaceutical) interventions. Currently, many studies investigate the prediction of the conversion from MCI to AD using feature sets similar to the ones used for the classification of subjects. A selection of these studies can be found in Table VII.

A. Prediction Based on VBM

Davatzikos *et al.* [114] used high-dimensional image analysis and pattern classification methods and proved that there was a subtle, distributed, structural pattern change in MCI subjects, which could be identified and measured before clinical symptoms. Their analysis included a number of MTL structures, the cingulate, and parts of the orbitofrontal cortex. Similar to [52] and [109], the CA1 area appeared to be more affected, and it showed more diagnostic accuracy from the total hippocampal volume. In contrast to [68], [69], and [72], where lateralized hippocampal atrophy was mainly observed, the study by Davatzikos *et al.* [114] indicated bilateral hippocampal atrophy. When the results were cross-validated, the analysis showed a 90% predictive power. In a more recent study by Davatzikos *et al.* [44], where VBM was used, a lower classification accuracy (56%) was achieved maybe due to the fact that the SVM was trained on NC and AD patients. In [99], Misra *et al.* used VBM analysis to evaluate the volume of WM and GM in 103 MCI subjects, which they were followed up for 15 months in order to predict, which individuals will convert to AD. They evaluated their results via cross-validation and achieved a classification accuracy of 82%. However, the number of progressive MCI patients was low ($N = 27$); thus, the results of this study are not directly comparable to other studies that used the ADNI image set. Plant *et al.* [45] used three different classifiers including SVM, Bayes, and voting feature intervals. When the anterior cingulate gyrus and orbitofrontal cortex were included in the measurements, the best predictive accuracy obtained was 75%. Duchesne *et al.* [122] used only MTL in their VBM analysis, and their results were better compared to other studies (see Table VII) that used the whole brain.

Koikkalainen *et al.* [123] used tensor-based morphometry (TBM) to classify stable from progressive MCI subjects. They selected ROIs using statistical maps of differences on their test set, and they achieved an overall accuracy of 72%. However, their results may be biased as the training and testing were not completely independent. Chételat *et al.* [46] longitudinally assessed (for 18 months) the possible structural changes in MCI patients and then compared these changes between the nonconverter and converter subjects. A fully automated VBM analysis was carried out, and results were similar to the changes observed by other VBM studies such as [105]. Interestingly, (perhaps due to methodological issues) in contrast with most of the ROI volume studies, they did not detect any hippocampal volume differences between AD and MCI patients, suggesting that a plateau has been reached.

B. Prediction Based on Volume Analysis

Chupin *et al.* [40] used an automated segmentation technique of the hippocampus and amygdala, and hippocampal volume was calculated to predict the conversion from MCI to AD. An overall classification accuracy of 64% was achieved, indicating that global hippocampal volume evaluation may not be an accurate measure for prognosis, mainly due to the fact that hippocampal volume is variable in young and older adults, which, in turn, may have implications on the final results [124].

The study by Tapiola *et al.* [125] used MCI patients who were followed-up for 34 months to investigate the predictive value of different methods on conversion from MCI to AD. They used MRI-derived volumes of MTL structures, WM lesions, MMSE scores, and APOE genotype. Interestingly, their results revealed that only MTL volume was able to predict the patients at high risk for developing the disease. Similar results were observed in the study by deToledo-Morrell *et al.* [97], where hippocampal and entorhinal cortex volumes were compared to determine which of the two regions could differentiate stable from progressive subjects. Twenty-seven MCI patients were followed after baseline diagnosis for 36 months, and ten of them converted to AD. The results showed that both hippocampus and entorhinal cortex could make the prediction; however, the entorhinal cortex was the best predictor with a rate of 93.5%.

Killiany *et al.* [12] investigated the most frequent ROIs used in volume analysis for the assessment of AD, the hippocampus, and the entorhinal cortex. Patients with mild AD at baseline were included as well. The measures between the two ROIs were different for each of the pairwise comparisons between the groups. The entorhinal cortex volume was able to differentiate the subjects that will probably develop the disease with an accuracy of 84%, whereas the hippocampal volume could not. The study suggested that more neuronal changes occur within the entorhinal cortex during the preclinical phase of AD, and as the disease spreads, atrophic changes develop within the hippocampus as well. Similarly to the study by Pennanen *et al.* [72], the hippocampal volume loss in MCI subjects was 8%, whereas, in entorhinal cortex, volume loss was almost double.

Devanand *et al.* [126] measured hippocampal and entorhinal cortex atrophy for the prediction of conversion from MCI to AD. In this large longitudinal study, 163 MCI patients and 63 NC subjects were followed for five years. Their results confirmed most of the findings of other studies that used smaller samples [12], [127], where hippocampal and entorhinal cortex had more atrophy in MCI converters to AD compared to NC and MCI nonconverters. Specifically, entorhinal cortex volume in converters was 17% lower than in nonconverters and 29% lower than in NC. For hippocampal volume, the percentages were 11% and 14%, respectively. Interestingly, it was observed that when both regions were used together with cognitive scores, the prediction accuracy was improved to 87.7%. Both hippocampal and entorhinal cortex volumes contributed to the prediction; however, the entorhinal cortex remained highly significant even after controlling for age and cognitive measures. On the other hand, hippocampal volume correlated with cognitive measures and, thus, less significant for prediction.

Killiany *et al.* [95] found that entorhinal cortex and superior temporal sulcus including the anterior cingulate gyrus (which is not yet known at which stage of the disease starts to involve) were the most useful regions for prediction of conversion to AD. These areas were used to determine if quantitative MRI measures at baseline could be used to determine whether subjects in the prodromal phase of the disease could be accurately identified before they develop AD. A discrimination accuracy of 93% between NC and the subjects with memory difficulty who eventually developed the disease was achieved. The discrimination

accuracy of the subjects with memory difficulty who did not developed the disease between the NC and the converters was 85% and 75%, respectively. Entorhinal cortex and the superior temporal sulcus ROIs were the best discriminators when NC were included.

C. Prediction Based on Thickness Analysis

Querbes *et al.* [66] used baseline normalized thickness index on a large sample of patients for the prediction of conversion from stable MCI to AD and compared it to the predictive values of the main cognitive scores at baseline. Their results showed that subtle structural changes could be detected and used to predict the outcome even two years before the clinical symptoms appear with a predictive value of 73%. This study had the advantage of using a cross-validation procedure. However, according to Eskildsen *et al.* [128], the results of the study most likely show an overestimated accuracy, as some subjects are used both for training and testing. Bakkour *et al.* [35] investigated the abnormalities of the cortex on patients with questionable AD and tried to detect which neocortical measures were better for early diagnosis and predictive power. A total of 49 questionable AD patients were longitudinally followed-up for 2.5 years, and according to their results, 20 patients converted to mild AD, while 29 remained stable. The MTL cortical thickness achieved the best performance.

In a very similar study [128], patterns of cortical thickness measurements were used for the prediction of AD. It was observed that atrophy patterns differed with the disease progression; thus, by learning these differences, the prediction accuracies could be improved. MCI subjects who had scans at 6, 12, 18, 24, and 36 months prior to the diagnosis of AD were selected from the ADNI database, and they were grouped into time-homogenous groups of progressive MCI. Then, these patients where compared with MCI subjects who remained stable during their longitudinal study period. Interestingly, it was noted that even at 36 months prior to the AD diagnosis, the hippocampus could not be used for prediction of the disease. On the other hand, the entorhinal cortex was the area affected first, followed by hippocampus. In other studies, such as [40], [44], [66], [99], and [129], the baseline data for analysis were not homogeneous with respect to the "time to conversion," since the progressive MCI patients would convert anytime over the course of six months to four years follow-up. According to the authors, such heterogeneity may conceal the neurodegenerative processes that could be attributed to the different substages of AD. For example, the pattern of atrophy could differ one year before diagnosis compared to the pattern two years earlier.

The study by Desikan *et al.* [130] identified MCI patients who converted to AD within two years after baseline with an overall accuracy of 91%. They used automated MRI-based software tools to compute measurements of MTL cortex thickness and volume on 64 ROIs among the two hemispheres of 324 MCI subjects. Furthermore, they compared their results with CSF samples and PET measures, and remarkably, they showed that structural MRI could better predict the disease progression. In a comparable study by Vemuri *et al.* [131], where structural MRI and CSF biomarkers on 399 subjects were used, the results were similar. It was found that the Structural Abnormality Index (STAND) score [38] could predict with higher accuracy the time to conversion compared to CSF.

D. Prediction Based on Shape Analysis

Costafreda *et al.* [32] used an automated procedure to extract 3-D hippocampal shape morphology. In their prediction model, only hippocampus was used, which achieved a predictive performance comparable or superior to other studies [45], [99], [122] that employed a multiregion or whole-brain approach. This was similar to the accuracy achieved using other predictive models based on nonautomated techniques. Similarly to [73] and [131], where morphometric pattern analysis was used, the results were significantly better from studies that suggested that 3-D shape analysis is better for the disease prognosis. Furthermore, this study and others [133]–[135] suggested that hippocampal head atrophy may be an early sign of risk and could be used to predict if a subject will develop the disease.

E. Multimethod Studies

Cuingnet *et al.* [30] compared most of the aforementioned methods used for classification. They obtained data from the ADNI database, and they used volume and shape analysis, VBM, and cortical thickness methods to predict the conversion to AD. By using SVM, they achieved predictive accuracies between 58% and 71%. In a similar pattern, Wolz *et al.* [129] used baseline scans from the entire MCI population of the ADNI cohort. Several methods were used for prediction obtaining accuracies in the range of 56–68%. When using the same subject groups with [30], they obtained better classification accuracies.

F. Prediction Using Texture Features

Sørensen *et al.* [81] tried to detect the accumulated effects caused by NFTs and Aβ plaques on the hippocampus as changes in the statistical properties of the images intensities. Furthermore, they tested the capability of hippocampal texture in the detection of early cognitive decline and whether texture analysis could reflect changes in hippocampal glucose metabolism in FDG-PET. Texture appeared to have higher but not significantly different AUC compared to hippocampal volume for the prediction of MCI to AD within 12 months. However, hippocampal texture was significantly better compared to volume, for the prediction of MCI to AD within 24 months, showing an AUC of $p = 0.005$ and $p = 0.002$, respectively. Interestingly, structural texture changes correlated with a reduction of glucose metabolism and the function of the hippocampus.

V. Concluding Remarks

Cerebral atrophy, as captured in structural MRI, is a promising biomarker in the assessment of early AD. Many studies [11], [72], [95], [136] proved that MTL is an area that showed atrophy even in the preclinical stage of the disease. Although hippocampal formation might be the most frequently used structure for the assessment of AD, the earlier involvement of the entorhinal

cortex was proved by many studies [12], [67], [68], [97], [101], [125], [137].

The necessity of quantitative MRI image processing and visualization derives from the fact that the human eye cannot perceive the subtle anatomical changes affecting the structures of the brain; thus, it detects atrophy after the brain has already undergone irreversible synaptic loss. All the aforementioned studies agree that medical image analysis is essential in the assessment of AD and can be used either for classification between subjects or for the prediction of conversion from MCI to AD.

A. Classification of MCI and AD Versus NC Subjects

1) Comparison of Hippocampus and Entorhinal Cortex in NC Versus AD Group: Overall, it appears that both entorhinal cortex and hippocampal volume classification accuracy is comparable in distinguishing NC subjects from AD patients. Both structures have similar reduction in atrophy. Furthermore, for this group, whole-brain approaches such as VBM and thickness remained competitive with hippocampal-based approaches, due to the fact that in the advance stages, atrophy is more widespread.

Shape analysis also gave very good results comparable to GM VBM for the classification between NC subjects and AD patients. However, the best classification accuracy (96.4%) for this group was reported by Zhang *et al.* [78] for texture analysis.

2) Comparison of Hippocampus and Entorhinal Cortex in NC Versus MCI Group: Both the hippocampus and entorhinal cortex can be used for the classification of patients between NC and MCI subjects. However, entorhinal cortex can provide better classification as it deteriorates earlier than hippocampus, which is consistent with many studies [9], [10], [57], [71], [125]. According to Gómez-Isla *et al.* [138], some entorhinal cortex layers can undergo 40% to 60% neuronal depopulation even in the earlier phase of AD. Indeed, the study by Pennanen *et al.* [72] revealed that the entorhinal cortex degenerated twice more rather than the hippocampus between NC and MCI. Thus, when AD patients are not included in the classification group, entorhinal cortex is the suggested structure to be used. All methods appear to have lower classification accuracy in this group of patients because, in MCI subjects, the changes are difficult to be identified. Shape analysis appears to be a better technique compared to volume analysis with similar results to voxel-based methods. However, to the best of our knowledge, the best classification accuracy (87%) mentioned in the literature between NC and MCI patients was achieved by Simoes *et al.* using texture features on the whole brain [36].

3) Comparison of Hippocampus and Entorhinal Cortex in MCI Versus AD Group: Both hippocampus and entorhinal cortex have the potential to discriminate MCI subjects from AD patients [70]. The study by Du *et al.* [71] suggested that the entorhinal cortex does not provide any further advantages for this classification. The study by Pennanen *et al.* [72] used hippocampal volume, but when they included entorhinal cortex to their model, the overall classification was not improved.

Shape analysis and VBM studies appear to have similar results for the classification between AD patients from NC and MCI versus AD. It is suggested that in the advanced stages of the disease, the atrophy is more widespread; thus, apart from ROI methods, whole-brain methods should be considered as well.

B. Prediction of Conversion From MCI to AD

Most of the studies [12], [67], [68], [97], [101], [125], [137] have been using quantitative MRI measures within the area of MTL to determine if a subject will develop the disease, and the results agree that entorhinal cortex is a better predictor compared to other structures such as the hippocampus. The best discrimination accuracy between normal and patients with memory difficulty, who eventually developed the disease, was achieved by two volume studies of deToledo-Morrell *et al.* [97] and Killiany *et al.* [95] with an overall predictive accuracy of 93.5% and 93%, respectively.

In the prediction of progression of the disease, the highest accuracies were achieved when both entorhinal cortex and hippocampus were combined in the analysis. VBM methods and cortical thickness gave lower accuracy compared to the other methods, and there is "lack of research" regarding the use of texture analysis in the prediction of progression from MCI to AD.

C. Conclusion

In conclusion, entorhinal cortex can provide better results in the classification of NC from MCI subjects, as the atrophy is more severe compared to the hippocampus in the early stages of the disease. For the discrimination accuracy of AD patients from NC and AD patients from MCI subjects, volumetric measurements of the hippocampus seem to be preferred mainly because entorhinal cortex is a very small region that is difficult to delineate when it is atrophied. Furthermore, image artifacts and/or anatomic ambiguities can obscure the boundaries of the entorhinal cortex. However, the hippocampus segmentation is more specific, and it provides more robust and accurate results for these two groups. On the other hand, entorhinal cortex is a better predictor of conversion from MCI to AD.

VI. Future Work

Nowadays, apart from classification, many researchers are concentrating in the prediction of the disease as well. It is very important to identify specific MRI diagnostic biomarkers to predict whether MCI subjects will eventually convert to AD patients. Perhaps, the initiation of serial MRI scans at annual or longer intervals to investigate the disease progression will provide insight in predicting the MCI subject that will develop the disease.

Interestingly, for the disease progression, with the use of medical image analysis, morphometric measures derived from structural MRI, can provide similar results with cellular or metabolic markers such as CSF, amyloid Aβ, and FDG-PET. A systematic and quantitative metaanalysis by Schroeter *et al.* [139] involved 1351 patients and 1097 NC from 40 studies. The aim of the study was to reveal the prototypical neural correlates of AD and its prodromal stage. The analysis included data from studies

that used structural MRI and studies that measured reduction in glucose utilization or in perfusion with PET. It was suggested that atrophy in the (trans-) entorhinal area/hippocampus and hypometabolism/hypoperfusion in the inferior parietal lobules could predict most reliably the progression from amnestic MCI to AD, although, in a metaanalysis [140], PET was a better disease predictor than MRI. However, there should be enough clinical information to justify irradiation of a subject, and this a major drawback for PET imaging. After the first symptoms appear, it was found that the evaluation and predictive accuracy was better using structural based biomarkers [131], [132], [141]. However, other studies [12], [72], [114] revealed that structural MRI can also be used before clinical symptoms appear, and in some cases, it could be more accurate rather than metabolic markers [130]–[132]. Marcus *et al.* [142] support that amyloid PET imaging should be perform in subjects with suspected AD because it was shown that Aβ plaques could also appear on nondemented elderly subjects. The presence of Aβ plaques in elderly nondemented subjects was also noticed in the study of Pike *et al.* [143]. Overall, the effectiveness of structural MRI compared to PET in predicting MCI conversion to AD is controversial.

Nowadays, medical image analysis has become a computationally rich process due to the additional new challenges, e.g., to predict if an MCI subject will convert to an AD patient. These processes include many intricate steps run on increasingly larger datasets with the use of many different tools. Graphical workflow environments such as LONI's Pipeline [29] facilitate numerous resources developed at other institutions such as FSL/Oxford [28] or Freesurfer/Harvard [25]. Combination of these tools can be used to analyze images efficiently and effectively. The advantages and possibilities of such workflow environments have not yet been investigated extensively.

In classification, the most challenging task appears to be the classification between NC and MCI subjects, as the classification accuracy of most of the studies is lower compared to other group of subjects (see Table VI). In the study by Davatzikos *et al.* [114], evaluation of WM areas of the brain both in the temporal lobe and in the superior and middle frontal gyri appeared to be necessary for the accurate classification of MCI subjects. However, apart from the hippocampus and entorhinal cortex, limited studies have investigated the aforementioned areas.

Imaging biomarkers are meaningless if they are not correlated with clinical assessment. The combination of two provides a better predictive accuracy [144]–[146]. It is also noted that are very few studies [30], [129] that combine volume, thickness, shape, intensity, and texture in multivariate assessment of the disease, which, in turn, may result to better classification and prediction accuracies. Martinez-Torteya *et al.* [80] used images from the ADNI database with their corresponding segmentation masks, provided by Heckemann *et al.* [147], to establish ROIs for every image. For each ROI, they used nine texture-related features together with 13 morphometrical features and 28 signal distribution related features. They revealed an MCI to AD progression biomarker, which yielded an AUC of 0.79. The same is true for the combination of imaging biomarkers derived from structural and functional imaging modalities [111], [148], as well as for the combination of MRI with genomic analysis toward personalized medicine and targeted drug development.

The use of texture analysis, especially of the 3-D texture, is also very restricted, when compared to the other methods, regarding the assessment of AD. However, some of the best classification accuracies were achieved with textures features [36], [78], [81], and it should be investigated more in the assessment of AD.

Research on the assessment of AD mainly involves volumetric 3-D T1-weighted sequences. However, there are several other MRI strategies such as diffusion weighted imaging, MRI, and diffusion tensor imaging [149] that have yet to be investigated in large cohort studies.

Finally, deep learning is the new trend in medical image analysis that is becoming the methodology of choice in many studies. Deep learning algorithms are based on neural networks of several layers of neurons, through which a signal is propagated and can also be used for segmentation, registration, classification, and other tasks in the assessment of AD [150].

Quantitative MRI can have a great impact in the assessment, evaluation, and treatment of AD especially if approaches described in this review move from the experimental stage to the clinical soon. Similarly, quantitative MRI biomarkers could also contribute in dementia differential diagnosis.

Acknowledgment

Conflict of interest: The authors declare that they have no conflict of interest.

References

[1] Alzheimer's Disease and Dementia | Alzheimer's Association, May 31, 2016. [Online]. Available: http://www.alz.org/
[2] H. Braak and E. Braak, "Staging of Alzheimer-related cortical destruction," *Int. Psychogeriatrics*, vol. 9, no. 1, pp. 257–261, 1997.
[3] C. R. Jack *et al.*, "Hypothetical model of dynamic biomarkers of the Alzheimer's pathological cascade," *Lancet Neurol.*, vol. 9, no. 1, pp. 119–128, Jan. 2010.
[4] M. F. Folstein, S. E. Folstein, and P. R. McHugh, "Mini-mental state". A practical method for grading the cognitive state of patients for the clinician," *J. Psychiatric Res.*, vol. 12, no. 3, pp. 189–198, Nov. 1975.
[5] J. C. Morris, "The Clinical Dementia Rating (CDR): Current version and scoring rules," *Neurology*, vol. 43, no. 11, pp. 2412–2414, Nov. 1993.
[6] B. Dubois *et al.*, "Research criteria for the diagnosis of Alzheimer's disease: Revising the NINCDS-ADRDA criteria," *Lancet Neurol.*, vol. 6, no. 8, pp. 734–746, Aug. 2007.
[7] R. I. Scahill, J. M. Schott, J. M. Stevens, M. N. Rossor, and N. C. Fox, "Mapping the evolution of regional atrophy in Alzheimer's disease: Unbiased analysis of fluid-registered serial MRI," *Proc. Nat. Acad. Sci. USA*, vol. 99, no. 7, pp. 4703–4707, Apr. 2002.
[8] L. R. Squire, C. E. L. Stark, and R. E. Clark, "The medial temporal lobe," *Annu. Rev. Neurosci.*, vol. 27, pp. 279–306, 2004.
[9] H. Braak and E. Braak, "Neuropathological stageing of Alzheimer-related changes," *Acta Neuropathol.*, vol. 82, no. 4, pp. 239–259, 1991.
[10] J. H. Kordower *et al.*, "Loss and atrophy of layer II entorhinal cortex neurons in elderly people with mild cognitive impairment," *Ann. Neurol.*, vol. 49, no. 2, pp. 202–213, Feb. 2001.
[11] B. C. Dickerson *et al.*, "MRI-derived entorhinal and hippocampal atrophy in incipient and very mild Alzheimer's disease," *Neurobiol. Aging*, vol. 22, no. 5, pp. 747–754, Oct. 2001.
[12] R. J. Killiany *et al.*, "MRI measures of entorhinal cortex vs hippocampus in preclinical AD," *Neurology*, vol. 58, no. 8, pp. 1188–1196, Apr. 2002.
[13] J. L. Cummings and G. Cole, "Alzheimer disease," *JAMA*, vol. 287, no. 18, pp. 2335–2338, May 2002.

[14] M. Á. Muñoz-Ruiz *et al.*, "Structural MRI in frontotemporal dementia: comparisons between hippocampal volumetry, tensor-based morphometry and voxel-based morphometry," *PloS One*, vol. 7, no. 12, 2012, Art. no. e52531.

[15] C. Möller *et al.*, "Different patterns of cortical gray matter loss over time in behavioral variant frontotemporal dementia and Alzheimer's disease," *Neurobiol. Aging*, vol. 38, pp. 21–31, Feb. 2016.

[16] *The Alzheimer's Disease Neuroimaging Initiative (ADNI)*. [Online]. Available: http://adni.loni.usc.edu/. Accessed on: Nov. 2017.

[17] J. Jovicich *et al.*, "Reliability in multi-site structural MRI studies: Effects of gradient non-linearity correction on phantom and human data," *NeuroImage*, vol. 30, no. 2, pp. 436–443, Apr. 2006.

[18] J. G. Sled, A. P. Zijdenbos, and A. C. Evans, "A nonparametric method for automatic correction of intensity nonuniformity in MRI data," *IEEE Trans. Med. Imag.*, vol. 17, no. 1, pp. 87–97, Feb. 1998.

[19] J. L. Gunter *et al.*, "Measurement of MRI scanner performance with the ADNI phantom," *Med. Phys.*, vol. 36, no. 6, pp. 2193–2205, Jun. 2009.

[20] D. S. Marcus, A. F. Fotenos, J. G. Csernansky, J. C. Morris, and R. L. Buckner, "Open access series of imaging studies (OASIS): Longitudinal MRI data in nondemented and demented older adults," *J. Cogn. Neurosci.*, vol. 22, no. 12, pp. 2677–2684, Dec. 2010.

[21] S. Lovestone *et al.*, "AddNeuroMed—The European collaboration for the discovery of novel biomarkers for Alzheimer's disease," *Ann. New York Acad. Sci.*, vol. 1180, pp. 36–46, Oct. 2009.

[22] E. E. Bron *et al.*, "Standardized evaluation of algorithms for computer-aided diagnosis of dementia based on structural MRI: The CADDementia challenge," *NeuroImage*, vol. 111, pp. 562–579, May 2015.

[23] J. Lötjönen *et al.*, "Fast and robust extraction of hippocampus from MR images for diagnostics of Alzheimer's disease," *NeuroImage*, vol. 56, no. 1, pp. 185–196, May 2011.

[24] K. O. Babalola *et al.*, "Comparison and evaluation of segmentation techniques for subcortical structures in brain MRI," in *Proc. Int. Conf. Med. Image Comput. Comput.-Assisted Intervention*, 2008, pp. 409–416.

[25] B. Fischl *et al.*, "Automatically parcellating the human cerebral cortex," *Cerebral Cortex*, vol. 14, no. 1, pp. 11–22, Jan. 2004.

[26] K. Van Leemput *et al.*, "Automated segmentation of hippocampal subfields from ultra-high resolution in vivo MRI," *Hippocampus*, vol. 19, no. 6, pp. 549–557, Jun. 2009.

[27] R. A. Morey *et al.*, "A comparison of automated segmentation and manual tracing for quantifying hippocampal and amygdala volumes," *NeuroImage*, vol. 45, no. 3, pp. 855–866, Apr. 2009.

[28] S. M. Smith *et al.*, "Advances in functional and structural MR image analysis and implementation as FSL," *NeuroImage*, vol. 23, no. 1, pp. S208–S219, 2004.

[29] I. Dinov *et al.*, "Neuroimaging study designs, computational analyses and data provenance using the LONI pipeline," *PloS One*, vol. 5, no. 9, Sep. 2010, Art. no. e13070.

[30] R. Cuingnet *et al.*, "Automatic classification of patients with Alzheimer's disease from structural MRI: A comparison of ten methods using the ADNI database," *NeuroImage*, vol. 56, no. 2, pp. 766–781, May 2011.

[31] R. S. Desikan *et al.*, "Automated MRI measures identify individuals with mild cognitive impairment and Alzheimer's disease," *Brain*, vol. 132, no. 8, pp. 2048–2057, Aug. 2009.

[32] S. G. Costafreda *et al.*, "Automated hippocampal shape analysis predicts the onset of dementia in mild cognitive impairment," *NeuroImage*, vol. 56, no. 1, pp. 212–219, May 2011.

[33] E. Westman *et al.*, "AddNeuroMed and ADNI: Similar patterns of Alzheimer's atrophy and automated MRI classification accuracy in Europe and North America," *NeuroImage*, vol. 58, no. 3, pp. 818–828, Oct. 2011.

[34] G. B. Karas *et al.*, "A comprehensive study of gray matter loss in patients with Alzheimer's disease using optimized voxel-based morphometry," *NeuroImage*, vol. 18, no. 4, pp. 895–907, Apr. 2003.

[35] A. Bakkour, J. C. Morris, and B. C. Dickerson, "The cortical signature of prodromal AD," *Neurology*, vol. 72, no. 12, pp. 1048–1055, Mar. 2009.

[36] R. L. Simoes, C. H. Slump, and A. M. van Cappellen van Walsum, "Using local texture maps of brain MR images to detect Mild Cognitive Impairment," in *Proc. 21st Int. Conf. Pattern Recognit.*, 2012, pp. 153–156.

[37] S. Klöppel *et al.*, "Automatic classification of MR scans in Alzheimer's disease," *Brain*, vol. 131, no. 3, pp. 681–689, Mar. 2008.

[38] P. Vemuri *et al.*, "Alzheimer's disease diagnosis in individual subjects using structural MR images: Validation studies," *NeuroImage*, vol. 39, no. 3, pp. 1186–1197, Feb. 2008.

[39] O. Colliot *et al.*, "Discrimination between Alzheimer disease, mild cognitive impairment, and normal aging by using automated segmentation of the hippocampus," *Radiology*, vol. 248, no. 1, pp. 194–201, Jul. 2008.

[40] M. Chupin *et al.*, "Fully automatic hippocampus segmentation and classification in Alzheimer's disease and mild cognitive impairment applied on data from ADNI," *Hippocampus*, vol. 19, no. 6, pp. 579–587, Jun. 2009.

[41] E. Gerardin *et al.*, "Multidimensional classification of hippocampal shape features discriminates Alzheimer's disease and mild cognitive impairment from normal aging," *NeuroImage*, vol. 47, no. 4, pp. 1476–1486, Oct. 2009.

[42] J. L. Whitwell *et al.*, "MRI patterns of atrophy associated with progression to AD in amnestic mild cognitive impairment," *Neurology*, vol. 70, no. 7, pp. 512–520, Feb. 2008.

[43] G. Chételat *et al.*, "Three-dimensional surface mapping of hippocampal atrophy progression from MCI to AD and over normal aging as assessed using voxel-based morphometry," *Neuropsychologia*, vol. 46, no. 6, pp. 1721–1731, 2008.

[44] C. Davatzikos, P. Bhatt, L. M. Shaw, K. N. Batmanghelich, and J. Q. Trojanowski, "Prediction of MCI to AD conversion, via MRI, CSF biomarkers, pattern classification," *Neurobiol. Aging*, vol. 32, no. 12, pp. 2322.e19–2322.e27, Dec. 2011.

[45] C. Plant *et al.*, "Automated detection of brain atrophy patterns based on MRI for the prediction of Alzheimer's disease," *Neuroimage*, vol. 50, no. 1, pp. 162–174, Mar. 2010.

[46] G. Chételat *et al.*, "Using voxel-based morphometry to map the structural changes associated with rapid conversion in MCI: A longitudinal MRI study," *NeuroImage*, vol. 27, no. 4, pp. 934–946, Oct. 2005.

[47] I. D. Dinov *et al.*, "Applications of the pipeline environment for visual informatics and genomics computations," *BMC Bioinformat.*, vol. 12, Jul. 2011, Art. no. 304.

[48] S. W. Moon *et al.*, "Structural brain changes in early-onset Alzheimer's disease subjects using the LONI pipeline environment," *J. Neuroimag.*, vol. 25, no. 5, pp. 728–737, Sep. 2015.

[49] M. J. Firbank, R. Barber, E. J. Burton, and J. T. O'Brien, "Validation of a fully automated hippocampal segmentation method on patients with dementia," *Human Brain Mapping*, vol. 29, no. 12, pp. 1442–1449, Dec. 2008.

[50] A. Mechelli, C. J. Price, K. J. Friston, and J. Ashburner, "Voxel-based morphometry of the human brain: Methods and applications," *Current Med. Imag. Rev.*, vol. 1, pp. 105–113, May 31, 2005. [Online]. Available: http://www.eurekaselect.com/60128/article

[51] F. Kurth, C. Gaser, and E. Luders, "A 12-step user guide for analyzing voxel-wise gray matter asymmetries in statistical parametric mapping (SPM)," *Nature Protocols*, vol. 10, no. 2, pp. 293–304, Feb. 2015.

[52] M. Afzali and H. Soltanian-Zadeh, "Comparison of voxel-based morphometry (VBM) and tractography of diffusion tensor MRI (DT-MRI) in temporal lobe epilepsy," in *Proc. 18th Iranian Conf. Elect. Eng.*, 2010, pp. 18–23.

[53] J. Ashburner and K. J. Friston, "Why voxel-based morphometry should be used," *NeuroImage*, vol. 14, no. 6, pp. 1238–1243, Dec. 2001.

[54] S. S. Keller and N. Roberts, "Voxel-based morphometry of temporal lobe epilepsy: An introduction and review of the literature," *Epilepsia*, vol. 49, no. 5, pp. 741–757, May 2008.

[55] W. J. P. Henneman *et al.*, "Hippocampal atrophy rates in Alzheimer disease: Added value over whole brain volume measures," *Neurology*, vol. 72, no. 11, pp. 999–1007, Mar. 2009.

[56] M. J. Nitzken, M. F. Casanova, G. Gimelfarb, T. Inanc, J. M. Zurada, and A. El-Baz, "Shape analysis of the human brain: A brief survey," *IEEE J. Biomed. Health Informat.*, vol. 18, no. 4, pp. 1337–1354, Jul. 2014.

[57] H. Braak and E. Braak, "Frequency of stages of Alzheimer-related lesions in different age categories," *Neurobiol. Aging*, vol. 18, no. 4, pp. 351–357, Aug. 1997.

[58] G. Castellano, L. Bonilha, L. M. Li, and F. Cendes, "Texture analysis of medical images," *Clin. Radiol.*, vol. 59, no. 12, pp. 1061–1069, Dec. 2004.

[59] A. Kassner and R. E. Thornhill, "Texture Analysis: A review of neurologic MR imaging applications," *Amer. J. Neuroradiol.*, vol. 31, no. 5, pp. 809–816, May 2010.

[60] V. A. Kovalev, F. Kruggel, H. J. Gertz, and D. Y. von Cramon, "Three-dimensional texture analysis of MRI brain datasets," *IEEE Trans. Med. Imag.*, vol. 20, no. 5, pp. 424–433, May 2001.

[61] K. Laws, Textured image segmentation, Defense Tech. Inf. Center, Fort Belvoir, VA, USA, Tech. Rep. ADA083283, 1980.

[62] X. Tang, "Texture information in run-length matrices," *IEEE Trans. Image Process.*, vol. 7, no. 11, pp. 1602–1609, Nov. 1998.

[63] C. C. Reyes-Aldasoro and A. Bhalerao, "Volumetric texture description and discriminant feature selection for MRI," *Inf. Process. Med. Imag.*, vol. 18, pp. 282–293, Jul. 2003.

[64] C. C. Reyes Aldasoro and A. Bhalerao, "Volumetric texture segmentation by discriminant feature selection and multiresolution classification," *IEEE Trans. Med. Imag.*, vol. 26, no. 1, pp. 1–14, Jan. 2007.

[65] C. C. Reyes-Aldasoro and A. H. Bhalerao, "Volumetric texture analysis in biomedical imaging," in *Biomedical Diagnostics and Clinical Technologies: Applying High-Performance Cluster and Grid Computing*, M. Pereira and M. Freire, Eds. Hershey, PA, USA: IGI Global, 2011, pp. 200–248.

[66] O. Querbes *et al.*, "Early diagnosis of Alzheimer's disease using cortical thickness: Impact of cognitive reserve," *Brain*, vol. 132, no. 8, pp. 2036–2047, Aug. 2009.

[67] C. Galton *et al.*, "Temporal lobe rating scale: Application to Alzheimer's disease and frontotemporal dementia," *J. Neurol. Neurosurg. Psychiatry*, vol. 70, no. 2, pp. 165–173, Feb. 2001.

[68] K. Juottonen, M. P. Laakso, K. Partanen, and H. Soininen, "Comparative MR analysis of the entorhinal cortex and hippocampus in diagnosing Alzheimer disease," *AJNR Amer. J. Neuroradiol.*, vol. 20, no. 1, pp. 139–144, Jan. 1999.

[69] M. P. Laakso *et al.*, "Hippocampus and entorhinal cortex in frontotemporal dementia and Alzheimer's disease: A morphometric MRI study," *Biol. Psychiatry*, vol. 47, no. 12, pp. 1056–1063, Jun. 2000.

[70] Y. Xu *et al.*, "Usefulness of MRI measures of entorhinal cortex versus hippocampus in AD," *Neurology*, vol. 54, no. 9, pp. 1760–1767, May 2000.

[71] A. T. Du *et al.*, "Magnetic resonance imaging of the entorhinal cortex and hippocampus in mild cognitive impairment and Alzheimer's disease," *J. Neurol. Neurosurg. Psychiatry*, vol. 71, no. 4, pp. 441–447, Oct. 2001.

[72] C. Pennanen *et al.*, "Hippocampus and entorhinal cortex in mild cognitive impairment and early AD," *Neurobiol. Aging*, vol. 25, no. 3, pp. 303–310, Mar. 2004.

[73] G. Chetelat and J.-C. Baron, "Early diagnosis of Alzheimer's disease: Contribution of structural neuroimaging," *NeuroImage*, vol. 18, no. 2, pp. 525–541, Feb. 2003.

[74] L. G. Apostolova *et al.*, "3D comparison of hippocampal atrophy in amnestic mild cognitive impairment and Alzheimer's disease," *Brain J. Neurol.*, vol. 129, no. Pt 11, pp. 2867–2873, Nov. 2006.

[75] L. Ferrarini, G. B. Frisoni, M. Pievani, J. H. C. Reiber, R. Ganzola, and J. Milles, "Morphological hippocampal markers for automated detection of Alzheimer's disease and mild cognitive impairment converters in magnetic resonance images," *J. Alzheimers Disease*, vol. 17, no. 3, pp. 643–659, 2009.

[76] N. Amoroso, R. Errico, and R. Bellotti, "PRISMA-CAD: Fully automated method for computer-aided diagnosis of dementia based on structural MRI data," in *Proc. MICCAI Workshop Challenge Comput.-Aided Diagnosis Dementia Struct. MRI Data*, 2014, pp. 16–23.

[77] P. A. Freeborough and N. C. Fox, "MR image texture analysis applied to the diagnosis and tracking of Alzheimer's disease," *IEEE Trans. Med. Imag.*, vol. 17, no. 3, pp. 475–479, Jun. 1998.

[78] J. Zhang, C. Yu, G. Jiang, W. Liu, and L. Tong, "3D texture analysis on MRI images of Alzheimer's disease," *Brain Imag. Behav.*, vol. 6, no. 1, pp. 61–69, Mar. 2012.

[79] M. S. de Oliveira *et al.*, "MR imaging texture analysis of the corpus callosum and thalamus in amnestic mild cognitive impairment and mild Alzheimer disease," *AJNR Amer. J. Neuroradiol.*, vol. 32, no. 1, pp. 60–66, Jan. 2011.

[80] A. Martinez-Torteya *et al.*, "Magnetization-prepared rapid acquisition with gradient echo magnetic resonance imaging signal and texture features for the prediction of mild cognitive impairment to Alzheimer's disease progression," *J. Med. Imag.*, vol. 1, no. 3, pp. 31005–31005, 2014.

[81] L. Sørensen *et al.*, "Early detection of Alzheimer's disease using MRI hippocampal texture," *Human Brain Mapping*, vol. 37, pp. 1148–1161, Dec. 2015.

[82] H. Xia *et al.*, "Texture analysis and volumetry of hippocampus and medial temporal lobe in patients with Alzheimer's disease," in *Proc. Int. Conf. Biomed. Eng. Biotechnol.*, 2012, pp. 905–908.

[83] X. W. Wei Fang Liu, "3D texture analysis of corpus caliosum based on MR images in patients with Alzheimer's disease and mild cognitive impairment," *Appl. Mech. Mater.*, vol. 533, pp. 415–420, 2014.

[84] X. Li, H. Xia, Z. Zhou, and L. Tong, "3D texture analysis of hippocampus based on MR images in patients with Alzheimer disease and mild cognitive impairment," in *Proc. 3rd Int. Conf. Biomed. Eng. Informat.*, 2010, vol. 1, pp. 1–4.

[85] X. Zhou, Z. Liu, Z. Zhou, and H. Xia, "Study on texture characteristics of hippocampus in MR images of patients with Alzheimer's Disease," in *Proc. 3rd Int. Conf. Biomed. Eng. Informat.*, 2010, vol. 2, pp. 593–596.

[86] C. Salvatore *et al.*, "Magnetic resonance imaging biomarkers for the early diagnosis of Alzheimer's disease: A machine learning approach," *Front. Neurosci.*, vol. 9, 2015, Art. no. 307.

[87] T.-Y. Kim, J. Son, and K.-G. Kim, "The recent progress in quantitative medical image analysis for computer aided diagnosis systems," *Healthcare Informat. Res.*, vol. 17, no. 3, pp. 143–149, Sep. 2011.

[88] M. Blas, S. Turk, and M. P. Pohar, "Comparison of logistic regression and linear discriminant analysis: A simulation study," *Metodološki Zvezki*, vol. 1, no. 1, pp. 143–161, 2004.

[89] V. N. Vapnik, "An overview of statistical learning theory," *IEEE Trans. Neural Netw.*, vol. 10, no. 5, pp. 988–999, Sep. 1999.

[90] L. Auria and R. A. Moro, "Support vector machines (SVM) as a technique for solvency analysis," DIW Berlin Discussion Paper No. 811, 2008.

[91] A. K. Jain, R. P. W. Duin, and J. Mao, "Statistical pattern recognition: A review," *IEEE Trans. Pattern Anal. Mach. Intell.*, vol. 22, no. 1, pp. 4–37, Jan. 2000.

[92] J. V. Tu, "Advantages and disadvantages of using artificial neural networks versus logistic regression for predicting medical outcomes," *J. Clin. Epidemiol.*, vol. 49, no. 11, pp. 1225–1231, Nov. 1996.

[93] R. A. Fisher, "The use of multiple measurements in taxonomic problems," *Ann. Human Genetics*, vol. 7, pp. 179–188, 1936.

[94] J. P. Lerch *et al.*, "Automated cortical thickness measurements from MRI can accurately separate Alzheimer's patients from normal elderly controls," *Neurobiol. Aging*, vol. 29, no. 1, pp. 23–30, Jan. 2008.

[95] R. J. Killiany *et al.*, "Use of structural magnetic resonance imaging to predict who will get Alzheimer's disease," *Ann. Neurol.*, vol. 47, no. 4, pp. 430–439, Apr. 2000.

[96] D. A. Freedman, *Statistical Models*. Cambridge, U.K.: Cambridge Univ. Press, 2009. [Online]. Available: http://www.goodreads.com/work/best_book/9620152-statistical-models-theory-and-practice

[97] L. deToledo-Morrell *et al.*, "MRI-derived entorhinal volume is a good predictor of conversion from MCI to AD," *Neurobiol. Aging*, vol. 25, no. 9, pp. 1197–1203, Oct. 2004.

[98] C. Cortes and V. Vapnik, "Support-vector networks," *Mach. Learn.*, vol. 20, no. 3, pp. 273–297.

[99] C. Misra, Y. Fan, and C. Davatzikos, "Baseline and longitudinal patterns of brain atrophy in MCI patients, and their use in prediction of short-term conversion to AD: Results from ADNI," *NeuroImage*, vol. 44, no. 4, pp. 1415–1422, Feb. 2009.

[100] M. C. Evans *et al.*, "Volume changes in Alzheimer's disease and mild cognitive impairment: Cognitive associations," *Eur. Radiol.*, vol. 20, no. 3, pp. 674–682, Mar. 2010.

[101] G. F. Busatto *et al.*, "A voxel-based morphometry study of temporal lobe gray matter reductions in Alzheimer's disease," *Neurobiol. Aging*, vol. 24, no. 2, pp. 221–231, Apr. 2003.

[102] K. Juottonen *et al.*, "Volumes of the entorhinal and perirhinal cortices in Alzheimer's disease," *Neurobiol. Aging*, vol. 19, no. 1, pp. 15–22, Feb. 1998.

[103] R. J. Killiany, M. B. Moss, M. S. Albert, T. Sandor, J. Tieman, and F. Jolesz, "Temporal lobe regions on magnetic resonance imaging identify patients with early Alzheimer's disease," *Arch. Neurol.*, vol. 50, no. 9, pp. 949–954, Sep. 1993.

[104] E. Braak, K. Griffing, K. Arai, J. Bohl, H. Bratzke, and H. Braak, "Neuropathology of Alzheimer's disease: What is new since A. Alzheimer?" *Eur. Arch. Psychiatry Clin. Neurosci.*, vol. 249, pp. 14–22, 1999.

[105] G. B. Karas *et al.*, "Global and local gray matter loss in mild cognitive impairment and Alzheimer's disease," *NeuroImage*, vol. 23, no. 2, pp. 708–716, Oct. 2004.

[106] N. Schuff *et al.*, "MRI of hippocampal volume loss in early Alzheimer's disease in relation to ApoE genotype and biomarkers," *Brain J. Neurol.*, vol. 132, no. Pt 4, pp. 1067–1077, Apr. 2009.

[107] J. H. Morra *et al.*, "Validation of a fully automated 3D hippocampal segmentation method using subjects with Alzheimer's disease mild cognitive impairment, and elderly controls," *NeuroImage*, vol. 43, no. 1, pp. 59–68, Oct. 2008.

[108] C. R. Jack *et al.*, "Medial temporal atrophy on MRI in normal aging and very mild Alzheimer's disease," *Neurology*, vol. 49, no. 3, pp. 786–794, Sep. 1997.

[109] M. Chupin *et al.*, "Anatomically constrained region deformation for the automated segmentation of the hippocampus and the amygdala: Method and validation on controls and patients with Alzheimer's disease," *NeuroImage*, vol. 34, no. 3, pp. 996–1019, Feb. 2007.

[110] L. Mosconi *et al.*, "Multicenter standardized 18F-FDG PET diagnosis of mild cognitive impairment, Alzheimer's disease, and other dementias," *J. Nucl. Med.*, vol. 49, no. 3, pp. 390–398, Mar. 2008.
[111] C. R. Jack *et al.*, "11C PiB and Structural MRI provide complementary information in imaging of AD and Amnestic MCI," *Brain J. Neurol.*, vol. 131, no. Pt 3, pp. 665–680, Mar. 2008.
[112] Y. Li *et al.*, "Regional analysis of FDG and PIB-PET images in normal aging, mild cognitive impairment, and Alzheimer's disease," *Eur. J. Nucl. Med. Mol. Imag.*, vol. 35, no. 12, pp. 2169–2181, Dec. 2008.
[113] G. W. Small *et al.*, "PET of brain amyloid and tau in mild cognitive impairment," *New Engl. J. Med.*, vol. 355, no. 25, pp. 2652–2663, Dec. 2006.
[114] C. Davatzikos, Y. Fan, X. Wu, D. Shen, and S. M. Resnick, "Detection of prodromal Alzheimer's disease via pattern classification of MRI," *Neurobiol. Aging*, vol. 29, no. 4, pp. 514–523, Apr. 2008.
[115] M. J. West, C. H. Kawas, W. F. Stewart, G. L. Rudow, and J. C. Troncoso, "Hippocampal neurons in pre-clinical Alzheimer's disease," *Neurobiol. Aging*, vol. 25, no. 9, pp. 1205–1212, Oct. 2004.
[116] G. B. Frisoni, F. Sabattoli, A. D. Lee, R. A. Dutton, A. W. Toga, and P. M. Thompson, "In vivo neuropathology of the hippocampal formation in AD: A radial mapping MR-based study," *NeuroImage*, vol. 32, no. 1, pp. 104–110, Aug. 2006.
[117] P. M. Szczypiński, M. Strzelecki, A. Materka, and A. Klepaczko, "MaZda—A software package for image texture analysis," *Comput. Methods Programs Biomed.*, vol. 94, no. 1, pp. 66–76, Apr. 2009.
[118] T. Kaeriyama, N. Kodama, T. Shimada, and I. Fukumoto, "Application of run length matrix to magnetic resonance imaging diagnosis of Alzheimer-type dementia," *Nihon Hōshasen Gijutsu Gakkai Zasshi*, vol. 58, no. 11, pp. 1502–1508, Nov. 2002.
[119] N. Kodama, Y. Kawase, and K. Okamoto, "Application of texture analysis to differentiation of dementia with lewy bodies from Alzheimer's disease on magnetic resonance images," in *Proc. World Congr. Med. Phys. Biomed. Eng.*, 2007, pp. 1444–1446.
[120] B. Reisberg *et al.*, "Stage-specific behavioral, cognitive, and in vivo changes in community residing subjects with age-associated memory impairment and primary degenerative dementia of the Alzheimer type," *Drug Develop. Res.*, vol. 15, nos. 2/3, pp. 101–114, Jan. 1988.
[121] S. T. Farias, D. Mungas, B. R. Reed, D. Harvey, and C. DeCarli, "Progression of mild cognitive impairment to dementia in clinic- vs community-based cohorts," *Arch. Neurol.*, vol. 66, no. 9, pp. 1151–1157, Sep. 2009.
[122] S. Duchesne, C. Bocti, K. De Sousa, G. B. Frisoni, H. Chertkow, and D. L. Collins, "Amnestic MCI future clinical status prediction using baseline MRI features," *Neurobiol. Aging*, vol. 31, no. 9, pp. 1606–1617, Sep. 2010.
[123] J. Koikkalainen *et al.*, "Multi-template tensor-based morphometry: Application to analysis of Alzheimer's disease," *NeuroImage*, vol. 56, no. 3, pp. 1134–1144, Jun. 2011.
[124] S. J. Lupien *et al.*, "Hippocampal volume is as variable in young as in older adults: Implications for the notion of hippocampal atrophy in humans," *NeuroImage*, vol. 34, no. 2, pp. 479–485, Jan. 2007.
[125] T. Tapiola *et al.*, "MRI of hippocampus and entorhinal cortex in mild cognitive impairment: A follow-up study," *Neurobiol. Aging*, vol. 29, no. 1, pp. 31–38, Jan. 2008.
[126] D. P. Devanand *et al.*, "Hippocampal and entorhinal atrophy in mild cognitive impairment: Prediction of Alzheimer disease," *Neurology*, vol. 68, no. 11, pp. 828–836, Mar. 2007.
[127] C. R. Jack *et al.*, "Brain atrophy rates predict subsequent clinical conversion in normal elderly and amnestic MCI," *Neurology*, vol. 65, no. 8, pp. 1227–1231, Oct. 2005.
[128] S. F. Eskildsen *et al.*, "Prediction of Alzheimer's disease in subjects with mild cognitive impairment from the ADNI cohort using patterns of cortical thinning," *NeuroImage*, vol. 65, pp. 511–521, Jan. 2013.
[129] R. Wolz *et al.*, "Multi-method analysis of MRI images in early diagnostics of Alzheimer's Disease," *PLoS ONE*, vol. 6, no. 10, Oct. 2011, Art. no. e25446.
[130] R. S. Desikan *et al.*, "Automated MRI measures predict progression to Alzheimer's disease," *Neurobiol. Aging*, vol. 31, no. 8, pp. 1364–1374, Aug. 2010.
[131] P. Vemuri *et al.*, "MRI and CSF biomarkers in normal, MCI, and AD subjects," *Neurology*, vol. 73, no. 4, pp. 294–301, Jul. 2009.
[132] G. B. Frisoni, N. C. Fox, C. R. Jack, P. Scheltens, and P. M. Thompson, "The clinical use of structural MRI in Alzheimer disease," *Nature Rev. Neurol.*, vol. 6, no. 2, pp. 67–77, Feb. 2010.
[133] J. G. Csernansky *et al.*, "Preclinical detection of Alzheimer's disease: Hippocampal shape and volume predict dementia onset in the elderly," *NeuroImage*, vol. 25, no. 3, pp. 783–792, Apr. 2005.
[134] L. G. Apostolova *et al.*, "Conversion of mild cognitive impairment to Alzheimer disease predicted by hippocampal atrophy maps," *Arch. Neurol.*, vol. 63, no. 5, pp. 693–699, May 2006.
[135] J. H. Morra *et al.*, "Automated mapping of hippocampal atrophy in 1-year repeat MRI data from 490 subjects with Alzheimer's disease, mild cognitive impairment, and elderly controls," *NeuroImage*, vol. 45, no. 1, pp. S3–S15, Mar. 2009.
[136] C. R. Jack *et al.*, "Prediction of AD with MRI-based hippocampal volume in mild cognitive impairment," *Neurology*, vol. 52, no. 7, pp. 1397–1403, Apr. 1999.
[137] T. Gómez-Isla *et al.*, "Neuronal loss correlates with but exceeds neurofibrillary tangles in Alzheimer's disease," *Ann. Neurol.*, vol. 41, no. 1, pp. 17–24, Jan. 1997.
[138] T. Gómez-Isla *et al.*, "Profound loss of layer II entorhinal cortex neurons occurs in very mild Alzheimer's disease," *J. Neurosci.*, vol. 16, no. 14, pp. 4491–4500, Jul. 1996.
[139] M. L. Schroeter, T. Stein, N. Maslowski, and J. Neumann, "Neural correlates of Alzheimer's disease and mild cognitive impairment: A systematic and quantitative meta-analysis involving 1351 patients," *NeuroImage*, vol. 47, no. 4, pp. 1196–1206, Oct. 2009.
[140] Y. Yuan, Z.-X. Gu, and W.-S. Wei, "Fluorodeoxyglucose-positron-emission tomography, single-photon emission tomography, and structural MR imaging for prediction of rapid conversion to Alzheimer disease in patients with mild cognitive impairment: A meta-analysis," *AJNR Amer. J. Neuroradiol.*, vol. 30, no. 2, pp. 404–410, Feb. 2009.
[141] C. R. Jack *et al.*, "Serial PIB and MRI in normal, mild cognitive impairment and Alzheimer's disease: Implications for sequence of pathological events in Alzheimer's disease," *Brain*, vol. 132, no. 5, pp. 1355–1365, May 2009.
[142] C. Marcus, E. Mena, and R. M. Subramaniam, "Brain PET in the Diagnosis of Alzheimer's Disease," *Clin. Nucl. Med.*, vol. 39, no. 10, pp. e413–e426, Oct. 2014.
[143] K. E. Pike *et al.*, "Beta-amyloid imaging and memory in non-demented individuals: Evidence for preclinical Alzheimer's disease," *Brain J. Neurol.*, vol. 130, no. Pt 11, pp. 2837–2844, Nov. 2007.
[144] D. P. Devanand *et al.*, "Hippocampal and entorhinal atrophy in mild cognitive impairment: Prediction of Alzheimer disease," *Neurology*, vol. 68, no. 11, pp. 828–836, Mar. 2007.
[145] C. R. Jack *et al.*, "Comparison of Different MRI brain atrophy rate measures with clinical disease progression in AD," *Neurology*, vol. 62, no. 4, pp. 591–600, Feb. 2004.
[146] V. Julkunen *et al.*, "Cortical thickness analysis to detect progressive mild cognitive impairment: A reference to Alzheimer's disease," *Dementia Geriatric Cognitive Disorders*, vol. 28, no. 5, pp. 404–412, 2009.
[147] R. A. Heckemann *et al.*, "Automatic morphometry in Alzheimer's disease and mild cognitive impairment," *Neuroimage*, vol. 56, no. 4, pp. 2024–2037, Jun. 2011.
[148] A. Martínez-Torteya, V. Treviño, and J. G. Tamez-Peña, "Improved diagnostic multimodal biomarkers for Alzheimer's disease and mild cognitive impairment," *BioMed Res. Int.*, vol. 2015, 2015, Art. no. 961314. [Online]. Available: https://www.hindawi.com/journals/bmri/2015/961314/
[149] L. Bracoud *et al.*, "DWI and DTI results on normal controls, MCI, and Alzheimer's disease subjects from the rosas study," *J. Alzheimers Assoc.*, vol. 11, no. 7, pp. P801–P802, Jul. 2015.
[150] Y. LeCun, Y. Bengio, and G. Hinton, "Deep learning," *Nature*, vol. 521, no. 7553, pp. 436–444, May 2015.

Authors' photographs and biographies not available at the time of publication.